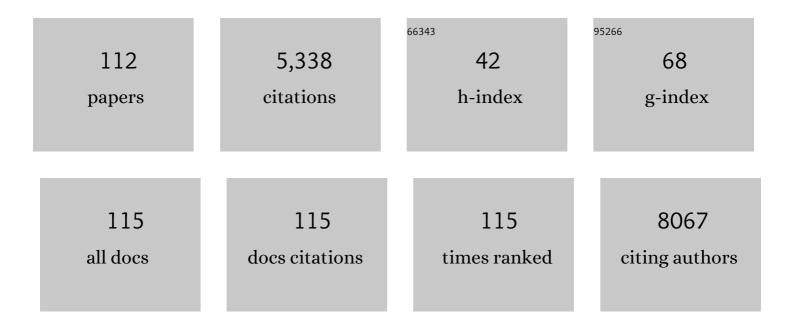
Chun-Gang Wang

List of Publications by Year in descending order

Source: https://exaly.com/author-pdf/1345026/publications.pdf Version: 2024-02-01



#	Article	IF	CITATIONS
1	Active targeted Janus nanoparticles enable anti-angiogenic drug combining chemotherapy agent to prevent postoperative hepatocellular carcinoma recurrence. Biomaterials, 2022, 281, 121362.	11.4	21
2	Designed formation of Prussian Blue/CuS Janus nanostructure with enhanced NIR-I and NIR-II dual window response for tumor thermotherapy. Journal of Colloid and Interface Science, 2022, 613, 671-680.	9.4	13
3	Enabling high-performance all-solid-state hybrid-ion batteries with a PEO-based electrolyte. Chemical Communications, 2022, 58, 6813-6816.	4.1	14
4	Achieving highly electrochemically active maricite NaFePO4 with ultrafine NaFePO4@C subunits for high rate and low temperature sodium-ion batteries. Chemical Engineering Journal, 2021, 405, 126689.	12.7	26
5	An EPR-independent therapeutic strategy: Cancer cell-mediated dual-drug delivery depot for diagnostics and prevention of hepatocellular carcinoma metastasis. Biomaterials, 2021, 268, 120541.	11.4	13
6	Amphiphilic Janus nanoparticles for imaging-guided synergistic chemo-photothermal hepatocellular carcinoma therapy in the second near-infrared window. Nanoscale, 2021, 13, 3974-3982.	5.6	14
7	Maximized Schottky Effect: The Ultrafine V ₂ O ₃ /Ni Heterojunctions Repeatedly Arranging on Monolayer Nanosheets for Efficient and Stable Waterâ€toâ€Hydrogen Conversion. Small, 2021, 17, e2005769.	10.0	42
8	Expediting the Conversion of Li ₂ S ₂ to Li ₂ S Enables High-Performance Li–S Batteries. ACS Nano, 2021, 15, 7318-7327.	14.6	101
9	Closeâ€packed storage of potassium metallic clusters achieved through nanostructure engineering of ultrafine hollow nanoparticlesâ€based carbon nanoclusters. EcoMat, 2021, 3, e12105.	11.9	7
10	Precise engineering of acorn-like Janus nanoparticles for cancer theranostics. Acta Biomaterialia, 2021, 130, 423-434.	8.3	7
11	Facile "Lotus Blooming―Strategy to Synthesize a 3D Carbon Nanosheet/Carbon Nanotube Framework with Embedded Co Nanocrystals for High-Performance Lithium–Sulfur Batteries. ACS Applied Energy Materials, 2021, 4, 11343-11352.	5.1	2
12	Biomolecules-assisted synthesis of degradable bismuth nanoparticles for dual-modal imaging-guided chemo-photothermal therapy. Chemical Engineering Journal, 2020, 382, 122720.	12.7	34
13	Highly dispersible hollow nanospheres organized by ultra-small ZnFe2O4 subunits with enhanced lithium storage properties. Journal of Alloys and Compounds, 2020, 812, 152014.	5.5	24
14	Construction of hierarchical yolk–shell nanospheres organized by ultrafine Janus subunits for efficient overall water splitting. Nanoscale, 2020, 12, 2578-2586.	5.6	14
15	Fluorescent silicon nanoparticles as dually emissive probes for copper(II) and for visualization of latent fingerprints. Mikrochimica Acta, 2020, 187, 65.	5.0	21
16	Tunable Synthesis of Mesoporous Prussian Blue@Calcium Phosphate Nanoparticles for Synergic Chemoâ€Photothermal Cancer Therapy. ChemistrySelect, 2020, 5, 10841-10847.	1.5	5
17	<i>in situ</i> engineered ultrafine NiS ₂ -ZnS heterostructures in micro–mesoporous carbon spheres accelerating polysulfide redox kinetics for high-performance lithium–sulfur batteries. Nanoscale, 2020, 12, 16201-16207.	5.6	28
18	Prussian Blue@Polyacrylic Acid/Au Aggregate Janus Nanoparticles for CT Imagingâ€guided Chemotherapy and Enhanced Photothermal Therapy. Advanced Therapeutics, 2020, 3, 2000091.	3.2	16

#	Article	IF	CITATIONS
19	Janus nanozyme–drug nanosystems for synergistic anti-inflammatory treatment of nasal polyps. CrystEngComm, 2020, 22, 7800-7807.	2.6	5
20	A simple synthesis of highly ordered microporous carbon nanospheres for high performance potassium-ion batteries. Journal of Power Sources, 2020, 479, 229113.	7.8	4
21	Rational design of well-dispersed ultrafine CoS ₂ nanocrystals in micro–mesoporous carbon spheres with a synergistic effect for high-performance lithium–sulfur batteries. Journal of Materials Chemistry A, 2020, 8, 10885-10890.	10.3	37
22	Co-delivery of hydrophilic/hydrophobic drugs by multifunctional yolk-shell nanoparticles for hepatocellular carcinoma theranostics. Chemical Engineering Journal, 2020, 389, 124416.	12.7	25
23	Nitrogen and Sulfur-Codoped Porous Carbon Nanospheres with Hierarchical Micromesoporous Structures and an Ultralarge Pore Volume for High-Performance Supercapacitors. ACS Applied Materials & Interfaces, 2020, 12, 8225-8232.	8.0	39
24	Ordered micro-mesoporous carbon spheres embedded with well-dispersed ultrafine Fe3C nanocrystals as cathode material for high-performance lithium-sulfur batteries. Chemical Engineering Journal, 2020, 388, 124315.	12.7	27
25	Sulfur@nitrogen-doped carbon yolk@shell nanospheres synthesized via in situ oxidation for Lithium–Sulfur batteries. Journal of Alloys and Compounds, 2020, 834, 155128.	5.5	15
26	Tailored synthesis of hollow MOF/polydopamine Janus nanoparticles for synergistic multi-drug chemo-photothermal therapy. Chemical Engineering Journal, 2019, 378, 122175.	12.7	68
27	Encapsulating Red Phosphorus in Ultralarge Pore Volume Hierarchical Porous Carbon Nanospheres for Lithium/Sodium-Ion Half/Full Batteries. ACS Nano, 2019, 13, 13513-13523.	14.6	77
28	Tunable synthesis of pH-responsive biodegradable ZnO nanospheres assembled from ultrasmall particles for cancer chemotherapy. Chemical Engineering Journal, 2019, 371, 443-451.	12.7	24
29	Facile synthesis of orange emissive carbon dots and their application for mercury ion detection and fast fingerprint development. Analytical Methods, 2019, 11, 2072-2081.	2.7	37
30	Engineering of Yin Yang-like nanocarriers for varisized guest delivery and synergistic eradication of patient-derived hepatocellular carcinoma. Nanoscale Horizons, 2019, 4, 1046-1055.	8.0	8
31	Multicolorful fluorescent-nanoprobe composed of Au nanocluster and carbon dots for colorimetric and fluorescent sensing Hg2+ and Cr6+. Sensors and Actuators B: Chemical, 2018, 262, 678-686.	7.8	80
32	Fabrication of a Flowerlike Ag Microsphere Film with Applications in Catalysis and as a SERS Substrate. European Journal of Inorganic Chemistry, 2018, 2018, 2835-2840.	2.0	14
33	Orange emissive carbon dots for colorimetric and fluorescent sensing of 2,4,6-trinitrophenol by fluorescence conversion. RSC Advances, 2018, 8, 16095-16102.	3.6	42
34	Nitrogen-doped carbon dots for the detection of mercury ions in living cells and visualization of latent fingerprints. New Journal of Chemistry, 2018, 42, 6824-6830.	2.8	54
35	Facile Approach to Synthesize Gold Nanorod@Polyacrylic Acid/Calcium Phosphate Yolk–Shell Nanoparticles for Dual-Mode Imaging and pH/NIR-Responsive Drug Delivery. Nano-Micro Letters, 2018, 10, 7.	27.0	45
36	Facile synthesis of bimetallic Ag-Cu nanoparticles for colorimetric detection of mercury ion and catalysis. Sensors and Actuators B: Chemical, 2018, 255, 1471-1481.	7.8	70

#	Article	IF	CITATIONS
37	Fluorescent silicon nanoparticles for sensing Hg2+ and Ag+ as well visualization of latent fingerprints. Dyes and Pigments, 2018, 149, 686-695.	3.7	61
38	A designed synthesis of multifunctional carbon nanoframes for simultaneous imaging and synergistic chemo-photothermal cancer therapy. New Journal of Chemistry, 2018, 42, 923-929.	2.8	12
39	Specific detection of latent human blood fingerprints using antibody modified NaYF4: Yb, Er, Gd fluorescent upconversion nanorods. Dyes and Pigments, 2018, 149, 822-829.	3.7	24
40	Uniform Pomegranateâ€Like Nanoclusters Organized by Ultrafine Transition Metal Oxide@Nitrogenâ€Doped Carbon Subunits with Enhanced Lithium Storage Properties. Advanced Energy Materials, 2018, 8, 1702347.	19.5	95
41	Tailored Surfaces on 2D Material: UFOâ€Like Cyclodextrinâ€Pd Nanosheet/Metal Organic Framework Janus Nanoparticles for Synergistic Cancer Therapy. Advanced Functional Materials, 2018, 28, 1803815.	14.9	82
42	Spadix-Bract Structured Nanobowls for Bimodal Imaging-Guided Multidrug Chemo-Photothermal Synergistic Therapy. Chemistry of Materials, 2018, 30, 3722-3733.	6.7	41
43	Selective Growth Synthesis of Ternary Janus Nanoparticles for Imaging-Guided Synergistic Chemo- and Photothermal Therapy in the Second NIR Window. ACS Applied Materials & Interfaces, 2018, 10, 24137-24148.	8.0	74
44	Dual drug delivery and sequential release by amphiphilic Janus nanoparticles for liver cancer theranostics. Biomaterials, 2018, 181, 113-125.	11.4	97
45	Uniform NiCo2O4/NiFe2O4 hollow nanospheres with excellent properties for Li-ion batteries and supercapacitors. Journal of Alloys and Compounds, 2018, 767, 223-231.	5.5	25
46	Single step synthesized three dimensional spindle-like nanoclusters as lithium-ion battery anodes. CrystEngComm, 2018, 20, 3043-3048.	2.6	3
47	Facile synthesis of polypyrrole@metal–organic framework core–shell nanocomposites for dual-mode imaging and synergistic chemo-photothermal therapy of cancer cells. Journal of Materials Chemistry B, 2017, 5, 1772-1778.	5.8	100
48	Designed Synthesis of Lipidâ€Coated Polyacrylic Acid/Calcium Phosphate Nanoparticles as Dual pHâ€Responsive Drugâ€Delivery Vehicles for Cancer Chemotherapy. Chemistry - A European Journal, 2017, 23, 6586-6595.	3.3	26
49	A stable pillared-layer Cu(<scp>ii</scp>) metal–organic framework with magnetic properties for dye adsorption and separation. New Journal of Chemistry, 2017, 41, 3661-3666.	2.8	33
50	Morphology tuning of assembled Au–Cu nicotinate rings by ligand coordination and their use as efficient catalysts. New Journal of Chemistry, 2017, 41, 1509-1517.	2.8	14
51	Rational Design of Branched Au–Fe ₃ O ₄ Janus Nanoparticles for Simultaneous Trimodal Imaging and Photothermal Therapy of Cancer Cells. Chemistry - A European Journal, 2017, 23, 17204-17208.	3.3	30
52	Precise synthesis of unique polydopamine/mesoporous calcium phosphate hollow Janus nanoparticles for imaging-guided chemo-photothermal synergistic therapy. Chemical Science, 2017, 8, 8067-8077.	7.4	125
53	One-pot controllable synthesis of CoFe ₂ O ₄ solid, hollow and multi-shell hollow nanospheres as superior anode materials for lithium ion batteries. Journal of Materials Chemistry A, 2017, 5, 21994-22003.	10.3	42
54	Designed Synthesis of Au/Fe ₃ O ₄ @C Janus Nanoparticles for Dualâ€Modal Imaging and Actively Targeted Chemoâ€Photothermal Synergistic Therapy of Cancer Cells. Chemistry - A European Journal, 2017, 23, 17242-17248.	3.3	55

#	Article	IF	CITATIONS
55	Facile one-pot synthesis of hollow mesoporous fluorescent Gd2O3:Eu/calcium phosphate nanospheres for simultaneous dual-modal imaging and pH-responsive drug delivery. Dyes and Pigments, 2017, 147, 514-522.	3.7	13
56	Tunable fabrication of folic acid-Au@poly(acrylic acid)/mesoporous calcium phosphate Janus nanoparticles for CT imaging and active-targeted chemotherapy of cancer cells. Nanoscale, 2017, 9, 14322-14326.	5.6	37
57	Near-infrared light and pH-responsive Au@carbon/calcium phosphate nanoparticles for imaging and chemo-photothermal cancer therapy of cancer cells. Dalton Transactions, 2017, 46, 14746-14751.	3.3	21
58	Rationally Designed Calcium Phosphate/Small Gold Nanorod Assemblies Using Poly(acrylic acid) Tj ETQq0 0 0 rgB Biomaterials Science and Engineering, 2017, 3, 3215-3221.	T /Overloo 5.2	ck 10 Tf 50 6 8
59	Facile preparation of fluorescent Au nanoclusters-based test papers for recyclable detection of Hg2+ and Pb2+. Sensors and Actuators B: Chemical, 2017, 241, 592-600.	7.8	68
60	One pot synthesis of highly fluorescent N doped C-dots and used as fluorescent probe detection for Hg2+ and Ag+ in aqueous solution. Sensors and Actuators B: Chemical, 2017, 243, 244-253.	7.8	97
61	A visible-light responsive zirconium metal–organic framework for living photopolymerization of methacrylates. RSC Advances, 2016, 6, 66444-66450.	3.6	18
62	SnO2@N-Doped Carbon Hollow Nanoclusters for Advanced Lithium-Ion Battery Anodes. European Journal of Inorganic Chemistry, 2016, 2016, 777-777.	2.0	0
63	A designed synthesis of multifunctional Fe ₃ O ₄ @carbon/zinc phosphate nanoparticles for simultaneous imaging and synergic chemo-photothermal cancer therapy. Journal of Materials Chemistry B, 2016, 4, 5809-5813.	5.8	21
64	Facile one-pot synthesis of carbon/calcium phosphate/Fe ₃ O ₄ composite nanoparticles for simultaneous imaging and pH/NIR-responsive drug delivery. Chemical Communications, 2016, 52, 11068-11071.	4.1	43
65	NIR-responsive NaYF 4 :Yb,Er,Gd fluorescent upconversion nanorods for the highly sensitive detection of blood fingerprints. Dyes and Pigments, 2016, 134, 178-185.	3.7	45
66	SnO ₂ @Nâ€Doped Carbon Hollow Nanoclusters for Advanced Lithiumâ€ion Battery Anodes. European Journal of Inorganic Chemistry, 2016, 2016, 812-817.	2.0	12
67	Tailored Synthesis of Octopusâ€type Janus Nanoparticles for Synergistic Activelyâ€Targeted and Chemoâ€Photothermal Therapy. Angewandte Chemie, 2016, 128, 2158-2161.	2.0	21
68	Tailored Synthesis of Octopusâ€ŧype Janus Nanoparticles for Synergistic Activelyâ€Targeted and Chemoâ€Photothermal Therapy. Angewandte Chemie - International Edition, 2016, 55, 2118-2121.	13.8	236
69	Facile approach to synthesize uniform Au@mesoporous SnO2 yolk–shell nanoparticles and their excellent catalytic activity in 4-nitrophenol reduction. Journal of Nanoparticle Research, 2016, 18, 1.	1.9	10
70	Electrical conductivity and electroluminescence of a new anthracene-based metal–organic framework with l€-conjugated zigzag chains. Chemical Communications, 2016, 52, 2019-2022.	4.1	102
71	Shape-controlled synthesis of 3D copper nicotinate hollow microstructures and their catalytic properties. RSC Advances, 2016, 6, 18033-18039.	3.6	9
72	Highly efficient visible-light-driven CO ₂ reduction to formate by a new anthracene-based zirconium MOF via dual catalytic routes. Journal of Materials Chemistry A, 2016, 4, 2657-2662.	10.3	231

#	Article	IF	CITATIONS
73	Nearâ€Infrared Light and pHâ€Responsive Polypyrrole@Polyacrylic acid/Fluorescent Mesoporous Silica Nanoparticles for Imaging and Chemoâ€Photothermal Cancer Therapy. Chemistry - A European Journal, 2015, 21, 16162-16171.	3.3	38
74	Facile Synthesis of Galactosamine‣tabilized Gold Nanoparticles with Sensitive Cd ²⁺ Sensing. European Journal of Inorganic Chemistry, 2015, 2015, 5656-5661.	2.0	4
75	Syntheses, structures, magnetic and luminescence properties of a series of coordination polymers constructed from 1,4-naphthalenedicarboxylate and N-donor ligands. CrystEngComm, 2015, 17, 4517-4524.	2.6	14
76	Designed preparation of polyacrylic acid/calcium carbonate nanoparticles with high doxorubicin payload for liver cancer chemotherapy. CrystEngComm, 2015, 17, 4768-4773.	2.6	34
77	Assembly of organic–inorganic hybrid materials constructed from polyoxometalate and metal–1,2,4-triazole units: synthesis, structures, magnetic, electrochemical and photocatalytic properties. CrystEngComm, 2015, 17, 2176-2189.	2.6	77
78	Facile and Scalable Synthesis of Novel Spherical Au Nanocluster Assemblies@Polyacrylic Acid/Calcium Phosphate Nanoparticles for Dualâ€Modal Imagingâ€Guided Cancer Chemotherapy. Small, 2015, 11, 3162-3173.	10.0	65
79	A combination of tri-modal cancer imaging and in vivo drug delivery by metal–organic framework based composite nanoparticles. Biomaterials Science, 2015, 3, 1270-1278.	5.4	130
80	Facile fabrication of hollow mesoporous Eu 3+ -doped Gd 2 O 3 nanoparticles for dual-modal imaging and drug delivery. Dyes and Pigments, 2015, 123, 8-15.	3.7	18
81	One pot synthesis of gold hollow nanospheres with efficient and reusable catalysis. RSC Advances, 2015, 5, 58522-58527.	3.6	22
82	Multifunctional spherical gold nanocluster aggregate@polyacrylic acid@mesoporous silica nanoparticles for combined cancer dual-modal imaging and chemo-therapy. Journal of Materials Chemistry B, 2015, 3, 2421-2425.	5.8	33
83	Cancer Therapy: Facile and Scalable Synthesis of Novel Spherical Au Nanocluster Assemblies@Polyacrylic Acid/Calcium Phosphate Nanoparticles for Dual-Modal Imaging-Guided Cancer Chemotherapy (Small 26/2015). Small, 2015, 11, 3082-3082.	10.0	3
84	Controlled synthesis of mesoporous hollow SnO ₂ nanococoons with enhanced lithium storage capability. Journal of Materials Chemistry A, 2015, 3, 22021-22025.	10.3	25
85	The facile synthesis of hollow Au nanoflowers for synergistic chemo-photothermal cancer therapy. Chemical Communications, 2015, 51, 14338-14341.	4.1	58
86	Silicaâ€Encapsulated Gd ³⁺ â€Aggregated Gold Nanoclusters for In Vitro and In Vivo Multimodal Cancer Imaging. Chemistry - A European Journal, 2014, 20, 8876-8882.	3.3	34
87	Fabrication of Au/ZnO nanoparticles derived from ZIF-8 with visible light photocatalytic hydrogen production and degradation dye activities. Dalton Transactions, 2014, 43, 16981-16985.	3.3	61
88	Hexamethylenetetramine-induced synthesis of hierarchical NiO nanostructures on nickel foam and their electrochemical properties. Journal of Alloys and Compounds, 2014, 603, 190-196.	5.5	27
89	Polyacrylic acid@zeolitic imidazolate framework-8 nanoparticles with ultrahigh drug loading capability for pH-sensitive drug release. Chemical Communications, 2014, 50, 1000-1002.	4.1	229
90	Fluorescent detection of TNT and 4-nitrophenol by BSA Au nanoclusters. Dalton Transactions, 2014, 43, 10057-10063.	3.3	104

#	Article	IF	CITATIONS
91	A novel strategy to fabricate multifunctional Fe3O4@C@TiO2 yolk–shell structures as magnetically recyclable photocatalysts. Nanoscale, 2014, 6, 6603.	5.6	33
92	Folic acid functionalized silver nanoparticles with sensitivity and selectivity colorimetric and fluorescent detection for Hg ²⁺ and efficient catalysis. Nanotechnology, 2014, 25, 355702.	2.6	30
93	Carbon nanodots@zeolitic imidazolate framework-8 nanoparticles for simultaneous pH-responsive drug delivery and fluorescence imaging. CrystEngComm, 2014, 16, 3259.	2.6	164
94	ZIF-8 templated fabrication of rhombic dodecahedron-shaped ZnO@SiO2, ZIF-8@SiO2 yolk–shell and SiO2 hollow nanoparticles. CrystEngComm, 2014, 16, 6534.	2.6	50
95	Conformational Supramolecular Isomerism in Two-Dimensional Fluorescent Coordination Polymers Based on Flexible Tetracarboxylate Ligand. Crystal Growth and Design, 2013, 13, 4092-4099.	3.0	46
96	Flowerlike Î ³ -Fe2O3@NiO hierarchical core-shell nanostructures as superb capability and magnetically separable adsorbents for water treatment. RSC Advances, 2013, 3, 12671.	3.6	18
97	Colorimetric detection of Hg2+ using thioctic acid functionalized gold nanoparticles. RSC Advances, 2013, 3, 24618.	3.6	39
98	Designed Fabrication of Unique Eccentric Mesoporous Silica Nanocluster-Based Core–Shell Nanostructures for pH-Responsive Drug Delivery. ACS Applied Materials & Interfaces, 2013, 5, 7282-7290.	8.0	72
99	Generalized Approach to the Synthesis of Reversible Concentric and Eccentric Polymerâ€Coated Nanostructures. Small, 2013, 9, 825-830.	10.0	43
100	Synergistic enhancement of photovoltaic performance of TiO2 photoanodes by incorporation of Dawson-type polyoxometalate and gold nanoparticles. Journal of Materials Chemistry, 2012, 22, 23627.	6.7	38
101	General Route to Multifunctional Uniform Yolk/Mesoporous Silica Shell Nanocapsules: A Platform for Simultaneous Cancerâ€7argeted Imaging and Magnetically Guided Drug Delivery. Chemistry - A European Journal, 2012, 18, 12512-12521.	3.3	118
102	Facile and fast synthesis of urchin-shaped Fe3O4@Bi2S3 core-shell hierarchical structures and their magnetically recyclable photocatalytic activity. Journal of Materials Chemistry, 2012, 22, 4832.	6.7	58
103	Controlled synthesis and magnetically separable photocatalytic properties of magnetic iron oxides@SnO2 yolk–shell nanocapsules. Journal of Materials Chemistry, 2012, 22, 13380.	6.7	20
104	Redox-active polyoxometalate-based crystalline material-immobilized noble metal nanoparticles: spontaneous reduction and synergistic catalytic activity. Journal of Materials Chemistry, 2012, 22, 21040.	6.7	22
105	Multifunctional fluorescent-magnetic polyethyleneimine functionalized Fe3O4–mesoporous silica yolk–shell nanocapsules for siRNA delivery. Chemical Communications, 2012, 48, 8706.	4.1	85
106	Selected ontrol Fabrication of Multifunctional Fluorescent–Magnetic Core–Shell and Yolk–Shell Hybrid Nanostructures. Chemistry - A European Journal, 2012, 18, 3745-3752.	3.3	27
107	Selected ontrol Synthesis of Monodisperse Fe ₃ O ₄ @C Core–Shell Spheres, Chains, and Rings as Highâ€Performance Anode Materials for Lithiumâ€Ion Batteries. Chemistry - A European Journal, 2012, 18, 11417-11422.	3.3	73
108	Uniform hollow mesoporous silica nanocages for drug delivery in vitro and in vivo for liver cancer therapy. Journal of Materials Chemistry, 2011, 21, 5299.	6.7	101

#	Article	IF	CITATIONS
109	Fluorescent hollow/rattle-type mesoporous Au@SiO2 nanocapsules for drug delivery and fluorescence imaging of cancer cells. Journal of Colloid and Interface Science, 2011, 358, 109-115.	9.4	72
110	L-cysteine functionalized gold nanoparticles for the colorimetric detection of Hg ²⁺ induced by ultraviolet light. Nanotechnology, 2010, 21, 025501.	2.6	154
111	Generalized Fabrication of Surfactant-Stabilized Anisotropic Metal Nanoparticles to Amino-Functionalized Surfaces: Application to Surface-Enhanced Raman Spectroscopy. Journal of Nanoscience and Nanotechnology, 2008, 8, 5887-5895.	0.9	7
112	Colorimetric detection of oligonucleotides using a polydiacetylene vesicle sensor. Analytical and Bioanalytical Chemistry, 2005, 382, 1708-1710.	3.7	85